Proc. Natl. Acad. Sci. USA
Vol. 96, pp. 3900–3905, March 1999
Medical Sciences

Choroid plexus epithelial expression of *MDR1* P glycoprotein and multidrug resistance-associated protein contribute to the blood–cerebrospinal-fluid drug-permeability barrier

VALLABHANENI V. RAO*†, JULIE L. DAHLHEIMER*†, MARK E. BARDGETT‡, ABRAHAM Z. SNYDER*, RICK A. FINCH§, ALAN C. SARTORELLI§, AND DAVID PIWNICA-WORMS*†¶

*Mallinckrodt Institute of Radiology, and †Departments of Molecular Biology and Pharmacology, and ‡Psychiatry, Washington University School of Medicine, St. Louis, MO 63110; and §Department of Pharmacology and Developmental Therapeutics Program, Yale University School of Medicine, New Haven, CT 06520

Communicated by Marcus E. Raichle, Washington University School of Medicine, St. Louis, MO, January 20, 1999 (received for review September 30, 1998)

ABSTRACT **The blood–brain barrier and a blood–cerebrospinal-fluid (CSF) barrier function together to isolate the brain from circulating drugs, toxins, and xenobiotics. The blood–CSF drug-permeability barrier is localized to the epithelium of the choroid plexus (CP). However, the molecular mechanisms regulating drug permeability across the CP epithelium are defined poorly. Herein, we describe a drug-permeability barrier in human and rodent CP mediated by epithelial-specific expression of the *MDR1* (multidrug resistance) P glycoprotein (Pgp) and the multidrug resistance-associated protein (MRP). Noninvasive single-photon-emission computed tomography with ^{99m}Tc-sestamibi, a membrane-permeant radiopharmaceutical whose transport is mediated by both Pgp and MRP, shows a large blood-to-CSF concentration gradient across intact CP epithelium in humans *in vivo*. In rats, pharmacokinetic analysis with ^{99m}Tc-sestamibi determined the concentration gradient to be greater than 100-fold. In membrane fractions of isolated native CP from rat, mouse, and human, the 170-kDa Pgp and 190-kDa MRP are identified readily. Furthermore, the murine proteins are absent in CP isolated from their respective *mdr1a/1b*(−/−) and *mrp*(−/−) gene knockout littermates. As determined by immunohistochemical and drug-transport analysis of native CP and polarized epithelial cell cultures derived from neonatal rat CP, Pgp localizes subapically, conferring an apical-to-basal transepithelial permeation barrier to radiolabeled drugs. Conversely, MRP localizes basolaterally, conferring an opposing basal-to-apical drug-permeation barrier. Together, these transporters may coordinate secretion and reabsorption of natural product substrates and therapeutic drugs, including chemotherapeutic agents, antipsychotics, and HIV protease inhibitors, into and out of the central nervous system.**

The *MDR1* (multidrug resistance) P glycoprotein (Pgp), implicated in chemotherapeutic failure when expressed in tumor cells, is expressed normally on apical membranes of a variety of cells derived from excretory tissues, as well as on the luminal surface of cerebral capillary endothelial cells (1, 2). The multidrug resistance-associated protein (MRP), a homologous ATP-binding cassette transporter implicated in cancer chemotherapeutic failure (3), also is expressed widely in various normal tissues, including epithelia (4). However, although MRP mRNA has been detected in whole-brain extracts (5), it is not expressed in brain capillaries; thus, the exact location and function of MRP in the central nervous system (CNS) remains unknown. Endothelial cells of cerebral capillaries, containing tight junctions and bipolar differential expression of transporters, maintain the blood–brain barrier (BBB). Recent data implicate Pgp as a critical component of the BBB, preventing entry and/or eliminating drugs and toxic compounds from the CNS (6, 7). However, morphometric studies of the choroid plexus (CP), a highly perfused and convoluted tissue projecting into the cerebrospinal fluid (CSF) of the ventricles, show an apical surface area in the same size range as the luminal surface area of the endothelial cells of the BBB (8), thereby providing an equally large surface for solute exchange. Thus, any Pgp-mediated component of the BBB confined to cerebral capillaries would be circumvented by a potential drug-permeation pathway across the CP, providing direct access to the CNS. However, it is known that the CP generally functions as a highly regulated solute- and drug-permeability barrier (9, 10). Because capillary endothelial cells of CP are fenestrated and lack both tight junctions and Pgp (2), permeation barriers within the CP must exist at the level of the epithelial cells lining the surface, although the molecular mechanisms of the broad-specificity transepithelial drug-permeability barrier within CP have just begun to be characterized. For example, a recently cloned multispecific transporter has been identified on the apical surface of CP epithelia (11). However, basolateral transporters remain to be identified. Because Pgp and MRP transport an overlapping but distinct array of structurally and functionally unrelated toxic xenobiotics, natural product drugs, phospholipids, and conjugated compounds (12), we hypothesized that Pgp and/or MRP might contribute directly to the blood–CSF (B-CSF) barrier of the CP.

MATERIALS AND METHODS

Cells and Protein Analysis. Pgp-expressing KB 8-5 cells and NIH 3T3 cells transfected with recombinant human *MDR1* were maintained in medium containing 10 ng/ml and 60 ng/ml colchicine (13), respectively, whereas NIH 3T3 cells transfected with recombinant human *MRP* were passaged once per month in 750 μg/ml G418 to maintain MRP expression (14). For immunoblots, crude membranes were prepared as described (4) from human CP (obtained from autopsy specimens within 12 h of death), adult rat (Sprague–Dawley) CP, KB 8-5 cells, and NIH 3T3 transfectants. Whole-cell lysates also were prepared from isolated CP of FVB *mdr1a/1b*(−/−) gene knockout mice (Taconic Farms; ref. 7), C57Bl/6 *mrp*(−/−) gene knockout mice (15), and their matched wild-type controls. Proteins were fractionated by SDS/PAGE and transferred to nitrocellulose; Pgp and MRP were detected with mAbs C219, C494, and QCRL-1 from Signet Laboratories (Dedham, MA) or with mAbs MRK16 and MRPr1 from Kamiya Biomedical (Thousand Oaks, CA) by using horseradish peroxidase-conjugated anti-mouse and anti-rat secondary

The publication costs of this article were defrayed in part by page charge payment. This article must therefore be hereby marked "*advertisement*" in accordance with 18 U.S.C. §1734 solely to indicate this fact.

PNAS is available online at www.pnas.org.

Abbreviations: BBB, blood–brain barrier; B-CSF, blood–cerebrospinal-fluid; CNS, central nervous system; CP, choroid plexus; CSF, cerebrospinal fluid; MRP, multidrug resistance-associated protein; Pgp, P glycoprotein; SPECT, single-photon-emission computed tomography.

¶To whom reprint requests should be addressed. e-mail: piwnica-worms@mirlink.wustl.edu.

antibodies with the enhanced chemiluminescence procedure (Amersham Pharmacia).

Immunohistochemistry. Frozen specimens of human CP autopsy material and brains of adult rat (Sprague–Dawley) were sectioned at thicknesses of 5 μm, air-dried, and fixed in either acetone at −20°C or 4% paraformaldehyde at room temperature for 10 min. Endogenous peroxidase was inactivated by incubation in 3% H_2O_2 in methanol for 30 min at room temperature. Histochemical detection was performed with the primary mAbs C219 (20 μg/ml), MRK16 (4 μg/ml), MRPr1 (1:20), or QCRL-1 (1:50) by using biotinylated anti-mouse or anti-rat IgG with ABC reagents (Vector Laboratories) according to the manufacturer's protocol, then counterstained with hematoxylin. Epitope-specific displacement of C219 against Pgp was performed by preincubation of the primary antibody for 1 h at 4°C with a 1,000-fold molar excess epitope-containing peptide, VVQEALDKAREGRTC (16). For all specimens, positive controls included 5-μm sections of pelleted, fresh-frozen KB 8-5-11 cells for Pgp and H69AR cells for MRP, respectively, mounted adjacent to the target tissue. Negative controls included adjacent sections of non-Pgp-expressing KB 3-1 cells and non-MRP-expressing H69 cells, respectively, and omission of the primary antibody.

Primary Cultures of CP Epithelial Cells. The CP was removed from the lateral and fourth ventricles of 1-week-old Sprague–Dawley neonatal rats and washed with Hanks' balanced salt solution. Epithelial cells were liberated by incubation at 37°C in Hanks' buffer containing pronase and type I DNase as described (17). Cells were plated on 10-mm Anocell tissue-culture inserts (Whatman Laboratories, Maidstone, U.K.) containing Anopore membranes (pore size of 0.2 μm) precoated with laminin (4 μg per insert) at a density of 7×10^5 cells per insert and incubated at 37°C in MEM (GIBCO) with D-valine, 15% dialyzed calf serum, 10 μg/ml gentamycin, 0.1% penicillin/streptomycin, and 2 mM glutamine in a humidified incubator with 5% CO_2. After 3 days of culture, medium was changed to Ham's F-12 and DMEM (1:1) with growth supplements as described (18), except that the medium also contained *cis*-hydroxyl proline (250 μg/ml) to prevent the growth of fibroblasts (19). Monolayers of epithelial cells were formed after 7–8 days in culture and used between day 9 and day 12.

Confocal Immunofluorescence and Electron Microscopy. Epithelial cells of rat CP cultured on Anopore culture inserts were washed in PBS, then fixed in acetone at −20°C for 10 min. Preparations were blocked in 1.5% horse serum (for Pgp) or goat serum (for MRP) in PBS, washed in serum-free PBS, and then incubated with mAbs C219 (10 μg/ml in PBS), MRPr1 (1:20), or NCL-ESA (anti-epithelial-specific antigen; 1:100, Novo Castra Labs). As secondary antibodies, fluorescein-labeled anti-mouse IgG (rat adsorbed) or anti-rat IgG (Vector Laboratories) were used. After staining, cells were overlaid with Vectashield (Vector) containing propidium iodide (1 μg/ml) and a glass coverslip, and then examined in planes from above the coverslip to below the insert with a laser-scanning confocal fluorescence imaging system (Model-2001 with IMAGESPACE software, Molecular Dynamics) coupled to a Nikon microscope and a computer. For electron microscopy, preparations were fixed, stained, cut, and viewed in a Zeiss EM902 electron microscope as described (20).

Functional Transport Assays. Primary monolayer cultures of 9- to 12-day-old neonatal rat CP epithelia that reached a peak resistance of >500 Ω/cm^2 (EVOM-G, World Precision Instruments, Sarasota, FL) were used for transport studies; 24-well tissue-culture plates, containing an experimental group of cell monolayers and a control group of inserts without cells, were used. Wells were washed twice with modified Earle's basic salt solution (MEBSS; ref. 21), and then Pgp inhibitor or vehicle was added to both sides of the monolayers for 15-min preincubation periods at 37°C. Each experiment was initiated by adding to either the apical side or the basal side of the cell layer 400 μl or 600 μl, respectively, of MEBSS containing ^{99m}Tc-sestamibi (DuPont; 10 pmol/mCi; 400 μCi/ml) or [^{3}H]Taxol (Moravek Biochemicals, Brea, CA; 10 Ci/mmol; 1 μCi/ml), as well as ^{14}C-labeled inulin (New England Nuclear; 1.92 mCi/g; 0.25 μCi/ml) with or without GF120918 (Glaxo Wellcome, 300 nM) or MK-571 (Merck Frosst Labs, Pointe Claire, PQ, Canada; 100 μM). At various times, aliquots of buffer were removed and counted for ^{99m}Tc or ^{3}H activity, as well as ^{14}C activity. Control experiments with Anopore membrane filters confirmed that nonspecific binding of tracers was <1% of added radioactivity (22). The appearance of radioactivity in the opposite compartment (trans) is presented as a fraction of total radioactivity added to the cis compartment.

***In Vivo* Microdialysis.** An 18-mm 20-g guide cannula (Small Parts, Miami) was implanted with a stereotaxic apparatus 1 mm above the left lateral ventricle (AP −1.0; ML −1.2; V 3.7) of adult male 250-g Sprague–Dawley rats as described (23). After a 3-day recovery to allow the BBB to reseal (24) and 1 day before the experiment, a concentric microdialysis probe was inserted through the in-dwelling cannula (25) into the lateral ventricle. Calibration experiments with the probe estimated an extraction fraction of 0.1 for experimental concentrations of radiolabeled drug. Animals received GF120918 (250 mg/kg of body weight) in vehicle (0.5% hydroxypropylmethylcellulose/1% Tween-80/distilled water) or vehicle alone administered by oral gavage 4 h before the injection of the radiopharmaceutical (13). For 2 h before the experiment and throughout the experiment, the probe was perfused with artificial cerebrospinal fluid [(in mM) 145 NaCl/2.7 KCl/1.0 $MgCl_2$/1.2 $CaCl_2$/2.0 $NaHPO_4$] at a flow rate of 0.5 μl/min with a syringe pump (Harvard 22, Harvard Apparatus). Animals were anesthetized with xylazine/ketamine (1.3 mg/8.7 mg per 100 g of body weight) and given supplemental doses as needed. After intravenous injection of ^{99m}Tc-sestamibi (100 mCi in 1 ml saline), concurrent brain microdialysate samples and periorbital venous samples of known volume were obtained at various time points and counted for γ-activity. On conclusion of each experiment, brains were harvested and sectioned with a freezing cryostat, and probe placement was verified by direct visual inspection of probe tracts in Nissl-stained coronal sections. Only animals with probes properly placed within the lateral ventricle were analyzed.

Human Imaging. All human studies were approved by an institutional review board. Gadolinium-chelate contrast-enhanced T1-weighted MRI were acquired with a 1.5T magnet by using a GE Signa MR scanner (TE = 11 ms; TR = 549 ms). Single-photon-emission computed tomography (SPECT) images were acquired starting 60 min after the intravenous injection of ^{99m}Tc-sestamibi (20 mCi) with a rotating dual-head camera (Genesys, Adac, Milpitas, CA) equipped with a low-energy high-resolution collimator with a 20% energy window centered over the 140-keV photopeak of ^{99m}Tc (1 eV = 1.602×10^{-19} J). SPECT data were coregistered with coronal MRI data by using a variant of an edge-detection algorithm (26).

RESULTS

B-CSF Permeability Barrier *in Vivo*. Analysis of the CNS distribution of ^{99m}Tc-sestamibi, a nonmetabolized radiopharmaceutical transported by both human Pgp and MRP (21, 27, 28), points to native CP functioning *in vivo* as a permeability barrier to agents in the multidrug-resistance phenotype. Localization by SPECT of radioactivity in human brain 90 min after injection of the agent was aligned anatomically by coregistration of the SPECT images with a high-resolution T1-weighted MRI of the head of the same volunteer (Fig. 1*A*). Although intense foci of radioactivity confined to the CP within each lateral ventricle of the brain were identified (29), there was no detectable activity in adjacent CSF or the surrounding brain parenchyma. Because ^{99m}Tc-sestamibi is otherwise freely diffusible across membrane bilayers and lacks significant binding to proteins and lipids (21), these images provide evidence for a carrier-mediated permeability barrier for ^{99m}Tc-sestamibi in human CP preventing entry of the agent into CSF.

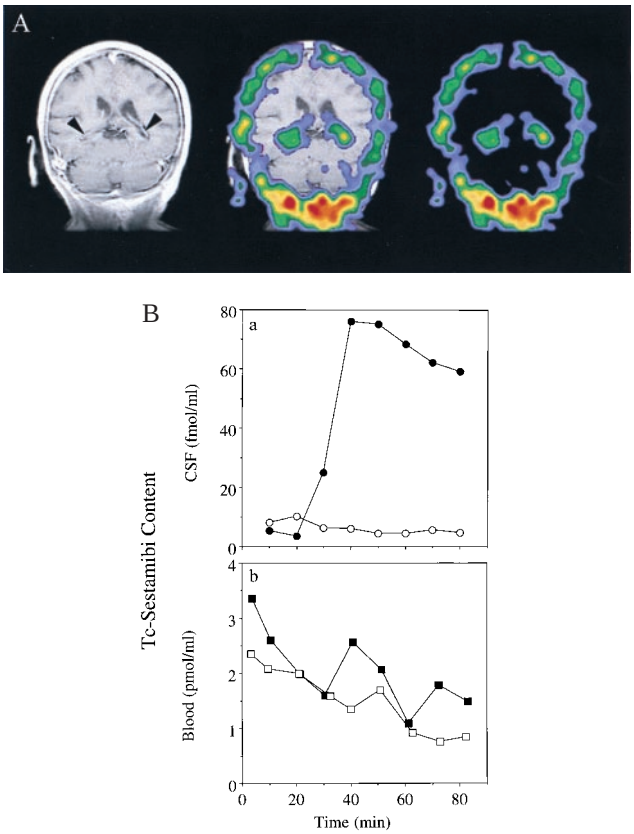

FIG. 1. Detection of B-CSF permeability barrier for ^{99m}Tc-sestamibi *in vivo* in human and rat. (*A*) Coronal human brain SPECT image 90 min after intravenous injection of ^{99m}Tc-sestamibi (*Right*); a gadolinium-chelate contrast-enhanced T1-weighted coronal head MRI (*Left*); and coregistered image (*Center*) of a human volunteer. Arrowheads on the MRI demarcate CP visualized bilaterally within the lateral ventricles. Note the radioactive drug localized to the CP. (*B*) In anesthetized rats, microdialysate samples from a cannulated lateral ventricle (○, ●) and concurrent blood samples from the periorbital plexus (□, ■) were collected at the indicated times after tail-vein injection of ^{99m}Tc-sestamibi in the absence (○, □) or presence of 250 mg/kg GF120918 (●, ■) and then counted for γ-activity. In the absence of GF120918, there is a 100-fold lower drug concentration in CSF compared with blood. Data represent a typical experiment from three independent experiments under each condition.

The magnitude of the ^{99m}Tc-sestamibi concentration gradient maintained across the B-CSF permeability barrier *in vivo* was quantified in a rat model. A cannula containing a microdialysis membrane was inserted through a burr hole into a lateral ventricle adjacent to the CP, and the disrupted BBB was allowed to reseal for 3 days. After tail-vein injection of ^{99m}Tc-sestamibi, radiotracer concentrations in CSF microdialysate samples were $<1/100$ of tracer concentrations concurrently measured in blood (Fig. 1*B*), consistent with the SPECT images. As a control experiment to assure detectability of the tracer in CSF under these conditions, animals were pretreated with GF120918 (250 mg/kg), a potent and specific inhibitor of Pgp (13, 30, 31). Subsequent intravenous injection of ^{99m}Tc-sestamibi resulted in a dramatic increase in the area under the concentration–time curve for tracer in CSF (Fig. 1*Ba*) without a significant change in blood (Fig. 1*Bb*; $P > 0.7$ for four experiments). Because multidrug-resistant (*mdr1a*) Pgp is expressed on the apical (luminal) surface of cerebral capillary endothelial cells, whereas ependymal cells lining the ventricles lack tight junctions, data from the inhibitor experiment confirmed the detectability of ^{99m}Tc-sestamibi in CSF, as the BBB was blocked. (As will be seen below, GF120918 does not enhance but rather inhibits basal-to-apical permeation through an isolated B-CSF barrier model.) The experiment also documented the time course of tracer back-diffusion from capillaries through CNS interstitial fluid into nascent CSF within the ventricles. Taken together, these experiments with intact organisms functionally illustrate that a large B-CSF permeability barrier to an multidrug-resistant agent is maintained normally in CP *in vivo*.

Western and Immunohistochemical Analysis of Native CP. Pgp was detected directly in enriched membrane fractions of both isolated human and rat CP by Western blot analysis with C219 (Fig. 2*A*), a mAb that recognizes an intracellular linear epitope present in all isoforms of Pgp (16). Pgp also was identified in human CP membrane fractions with C494 (data not shown), a mAb that detects an intracellular linear epitope present in only class 1 isoforms of Pgp (16). Furthermore, Pgp was identified (C219) in cell lysates of CP isolated from FVB wild-type mice but was not detectable in CP isolated from their *mdr1a/1b*(−/−) gene knockout (7) littermates (Fig. 2*A*). To localize the antigen further, immunohistochemical analysis (C219) of rat brain was performed. In CP, Pgp expression was confined to the epithelial cells (Fig. 2*B*). Analysis of the same specimens also confirmed the reported expression of Pgp in cerebral capillary endothelial cells (2). Furthermore, staining of human CP tissue with MRK16, a mAb that recognizes an extracellular epitope specific to human *MDR1* Pgp (32), showed a homogeneous expression pattern of *MDR1* Pgp confined to CP epithelial cells (Fig. 2*B*). Human CP epithelial cell-specific expression also was confirmed by peptide-displaceable staining with C219 (data not shown).

Similarly, MRP was detected by Western analysis of enriched membrane fractions of isolated human and rat CP with two different mAbs (Fig. 2*A*). The mAb MRPr1 recognizes an epitope present in both rodents and humans (33), whereas mAb QCRL-1 detects an epitope specific to human MRP1 (34). Furthermore, MRP was identified (MRPr1) in cell lysates of CP isolated from C57Bl/6 wild-type mice but was not detectable in CP isolated from their *mrp*(−/−) gene knockout (15) littermates (Fig. 2*A*). As shown in Fig. 2*C*, immunohistochemical staining (MRPr1) of rat brain showed expression of MRP restricted to the CP epithelial cells. Many areas showed a strong staining pattern preferentially localized basolaterally. In addition, staining of human CP tissue with either MRPr1 or QCRL-1 indicated that MRP expression was confined to CP epithelial cells (Fig. 2*C*).

Fluorescent Confocal and Electron Microscopy of CP Epithelial Cells in Culture. To characterize the polarity of Pgp and MRP expression further, primary cultures of CP epithelial cells obtained from neonatal rat were established and grown on Anopore membrane filters. Formation of confluent monolayers of cells with tight junctions and apical microvilli, features characteristic of native CP epithelia *in vivo* (18, 35), was confirmed by electron microscopy (Fig. 3). Furthermore, indirect immunofluorescence analysis with mAb NCL-ESA of cultured epithelial cells confirmed the uniform expression of epithelial-specific antigen (data not shown), further documenting maintenance of epithelial differentiation in culture. In 9- to 12-day-old cultures, indirect immunofluorescence (mAb C219) with confocal microscopy detected Pgp with a punctate or granular staining pattern throughout the cytoplasm (Fig. 4*A*). As reported for certain multidrug-resistant cells (36), this staining pattern was suggestive of a vesicular localization compartment for Pgp. A plasma-membrane expression pattern was occasionally, although not uniformly, observed. Confocal examination in planes perpendicular to the membrane filter showed staining for Pgp with a predominantly subapical distribution, although areas of scattered intracellular punctate foci and occasional basolateral foci were observed (Fig. 4*A*). Serial analysis of planes parallel to the culture surface also were consistent with a subapical predominance for Pgp expression (data not shown).

Indirect immunofluorescence with mAb MRPr1 applied to cultured CP epithelial cells showed an intense mosaic pattern of staining for MRP (Fig. 4*B*). MRP was expressed more obviously in a plasma membrane pattern than Pgp. Confocal examination in planes perpendicular to the membrane filter showed a strong preferential localization of expression of MRP toward the baso-

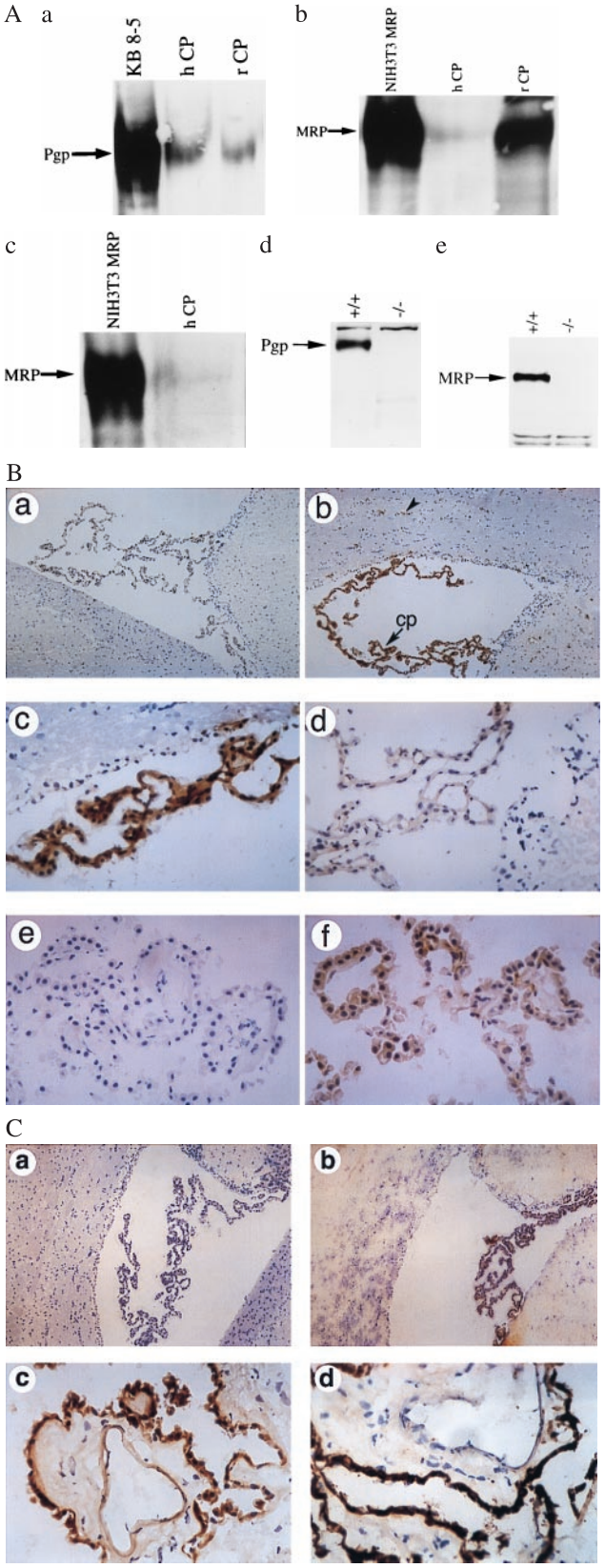

FIG. 2. (*A*) Expression of Pgp and MRP (arrows) in enriched membrane fractions of CP from rat (rCP) and human (hCP) shown by immunoblotting with C219 (*a*), MRPr1 (*b*), and QCRL-1 (*c*). Disruption of Pgp and MRP expression in cell lysates of CP isolated from FVB *mdr1a/1b*(−/−) and C57Bl/6 *mrp*(−/−) gene knockout mice, respectively, compared with their wild-type littermates shown by immunoblotting with C219 (*d*) and MRPr1 (*e*). C219 detects a protein of 170 kDa that comigrates with *MDR1* Pgp expressed in human multidrug-resistant KB 8-5 cells, whereas MRPr1 and QCRL-1 detect a protein of 190 kDa that comigrates with recombinant human MRP expressed in NIH 3T3 fibroblasts. In all lanes 50 μg of protein was used, except for NIH 3T3 MRP (25 μg). (*B*) Localization of Pgp to epithelial cells of rat and human CP by immunohistochemistry. Frozen rat brain tissue is stained in the absence of primary mAb (*a*; ×100), with mAb C219 (*b*; ×100), or with C219 (*c*; ×400); staining is abolished competitively by pre-equilibrating C219 in a 1,000-fold molar excess of a synthetic epitope-specific blocking peptide (*d*; VVQEALDKAREGRTC; ×400). Frozen human CP is stained in the absence of primary mAb (*e*; ×400) and in the presence of mAb MRK16 (*f*; ×400). Human CP epithelial cell-specific expression also was confirmed by peptide-displaceable staining with C219 (data not shown). (*b*) cp, CP within a lateral ventricle; the arrowhead indicates expression of Pgp in the capillary endothelial cells of rat brain parenchyma. (*C*) Localization of MRP to epithelial cells of rat and human CP by immunohistochemistry. Rat-brain sections immunostained in the absence of primary mAb (*a*; ×100) and in the presence of mAb MRPr1 (*b*; ×100). Human CP tissue stained with mAb MRPr1 (*c*; ×400) and mAb QCRL-1 (*d*; ×400).

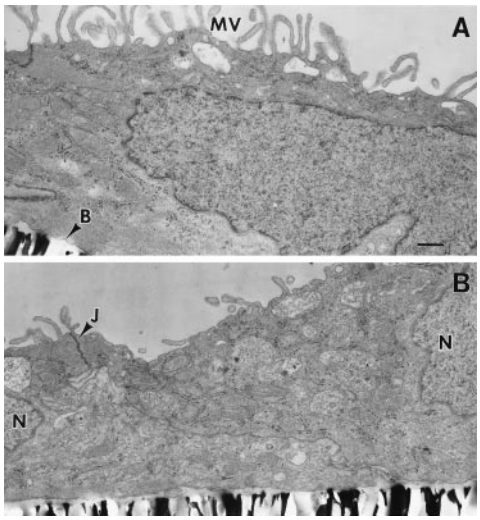

FIG. 3. Conventional electron microscopy of monolayers of cultured neonatal rat CP epithelial cells. Note abundant apical microvilli on the apical surface (*A*), the formation of basement membrane adjacent to the filter, and desmosomes between cells near their apical surfaces (*B*), features characteristic of native CP epithelia *in vivo* (18). MV, microvilli; B, basement membrane; N, nucleus; J, desmosome/tight junction complex. (Bar = 0.5 μm.)

lateral surface (Fig. 4*B*). Serial analysis of planes parallel to the culture surface confirmed a basolateral predominance for MRP expression (data not shown).

Transport Assays. Whether Pgp and MRP vectorially contribute to a CP transepithelial permeation barrier also was investigated with the primary rat CP epithelial cell model grown in confluent monolayers on filters in a transwell configuration. Only monolayers concurrently possessing high transepithelial electrical resistance (>500 Ω/cm^2) and low paracellular fluxes (transepithelial transport of <2%/h of [^{14}C]inulin) were used for transwell drug studies (18). As expected, CP epithelial cells on the filters formed a bidirectional diffusion barrier for ^{99m}Tc-sestamibi, reducing apical-to-basal and basal-to-apical permeation of the probe to 24% and 21%, respectively, of that found with filters alone during the first 15 min. Because ^{99m}Tc-sestamibi can diffuse freely and rapidly across membrane bilayers lacking carrier proteins and concentrate within intracellular electronegative compartments, such as mitochondria (21), vectorial transepithelial translocation of the drug is a result of the combined effects of passive diffusion in response to the electrochemical polarity of the epithelial layer, cellular accumulation, and any Pgp- or MRP-mediated transport. Of this transepithelial permeation of ^{99m}Tc-sestamibi, greater basal-to-apical than apical-to-basal translocation was detected (up to 2-fold greater by 3 h; Fig. 5*A*). Apical-

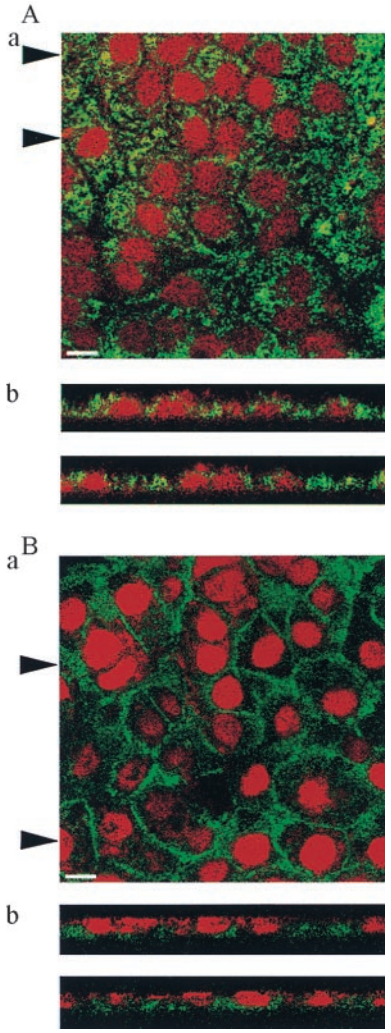

FIG. 4. Localization of Pgp expression with mAb C219 (*A*) and MRP expression with mAb MRPr1 (*B*) in cultured neonatal rat CP epithelial cells by confocal microscopy. (*Aa* and *Ba*) Top view of the cell layer. (Bar = 10 μm.) (*Ab and Bb*) Optical sections perpendicular to the plane of the cell layer. Arrowheads in *Aa* and *Ba* indicate positions of the respective sections in *Ab and Bb*. Pgp localizes predominantly toward apical surfaces, whereas MRP localizes toward basolateral surfaces.

to-basal permeation of ^{99m}Tc-sestamibi was significantly enhanced by adding the Pgp antagonist GF120918 at 300 nM, a maximal inhibitory concentration (13, 30), to both sides of the chamber. Conversely, GF120918 inhibited basal-to-apical permeation. The vectorial differences in drug permeation and in the effects of a Pgp-specific antagonist provide evidence for a Pgp-mediated permeability barrier localized to the apical surface. In addition, determination of total radioactivity associated with CP epithelial cells after 3-h incubations with ^{99m}Tc-sestamibi showed a typical GF120918-inducible increase in the net accumulation of ^{99m}Tc-sestamibi (3-fold by 3 h), consistent with prior results in cells transfected with *MDR1* Pgp (13), regardless of whether radioactivity was added to the apical or the basolateral side (Table 1).

We also tested the effects of MK-571 (37), a modulator reported to inhibit MRP transport activity in cells at high concentrations (12), on ^{99m}Tc-sestamibi translocation across CP epithelial cells. Control experiments with MK-571 (100 μM) that used ^{99m}Tc-sestamibi for transport analysis (13, 21) were performed in nonpolar NIH 3T3 cells stably transfected with human *MDR1* Pgp (38) or MRP (14). MK-571 was confirmed to mediate strong preferential transport inhibition of MRP over *MDR1* Pgp at the concentration tested. The enhancement after 30 min of cellular accumulation of ^{99m}Tc-sestamibi in the presence of MK-571 over control was, for NIH 3T3, 4-fold; for NIH 3T3 *MDR1*, 7-fold; and for NIH 3T3 *MRP*, 21-fold (n = 4 each). In contrast to GF120918, MK-571 slightly enhanced, rather than inhibited, basal-to-apical translocation of ^{99m}Tc-sestamibi. Furthermore, net enhancement of apical-to-basal permeation was not observed during the first 60 min of observation (Fig. 5*B*). These findings are consistent with inhibition of MRP on the basolateral surface. A 2-fold enhancement of final CP epithelial cell content of ^{99m}Tc-sestamibi was observed with MK-571 (Table 1), consistent with expectations for the inhibition of MRP. Specific inhibition of an MRP-mediated permeation barrier was not possible with other currently available inhibitors; probenecid (10 mM), sulfinpyrazone (1 mM), and genistein (100 μM), putative inhibitors of MRP, depolarized membrane potentials or were otherwise toxic to cultured CP epithelial cells at these concentrations.

Transwell permeation experiments also were performed with [^{3}H]Taxol, a cytotoxic agent for which transfection of *MDR1* and drug conditioning confers high levels of resistance (39), whereas transfection of *MRP* and conditioning confers no resistance (40); these findings are consistent with preferential Pgp-mediated transport of Taxol relative to MRP. CP epithelial cells grown on filters formed a bidirectional diffusion barrier for [^{3}H]Taxol, reducing apical-to-basal and basal-to-apical permeation of the probe to 4% and 9%, respectively, of that found with blank filters. Of this transcellular drug permeation, greater basal-to-apical than apical-to-basal translocation of the drug was observed (Fig. 5*c*). Simultaneous addition of the inhibitor GF120918 to both

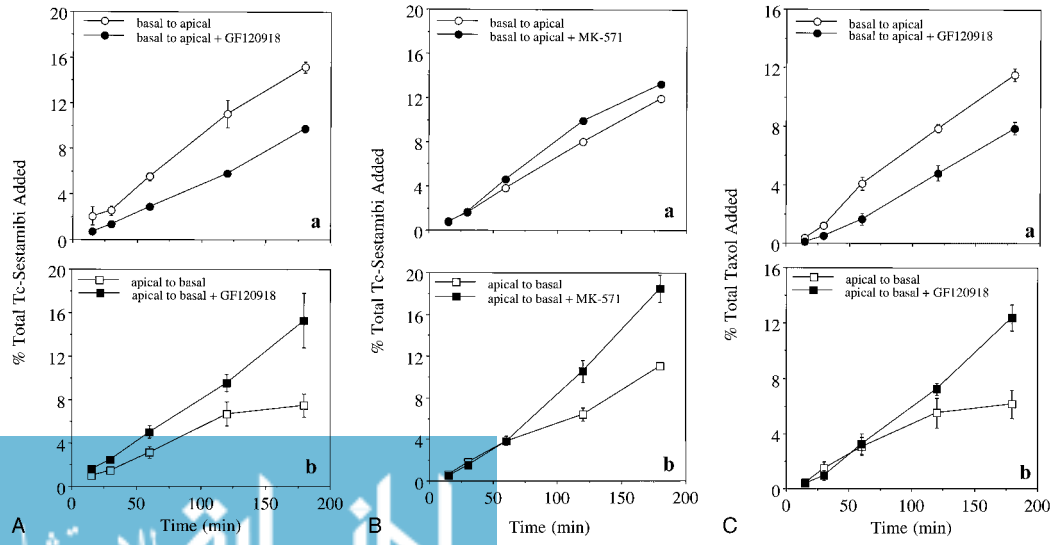

FIG. 5. Transepithelial transport of ^{99m}Tc-sestamibi and [^{3}H]Taxol across confluent monolayers of rat CP epithelial cells, wherein drug is added to either the basal (*Aa, Ba,* and *Ca*) or the apical (*Ab, Bb,* and *Cb*) side of the monolayers. (*A*) ^{99m}Tc-sestamibi added in the absence and presence of GF120918 (300 nM). (*B*) ^{99m}Tc-sestamibi added in the absence and presence of MK-571 (100 μM). (*C*) [^{3}H] Taxol added in the absence and presence of GF120918 (300 nM). Each point represents the mean value of three monolayers; bars represent ±SEM when larger than the symbol.

Table 1. Effect of modulators on net content of MDR transport substrates in cultured rat choroid plexus epithelial cells

	GF120918				MK-571			
	Basal		Apical		Basal		Apical	
Radioprobe	−	+	−	+	−	+	−	+
^{99m}Tc-sestamibi	0.85 ± 0.04	3.04 ± 0.15**	0.93 ± 0.08	3.34 ± 0.07**	1.39 ± 0.02	2.24 ± 0.21*	2.14 ± 0.13	4.19 ± 0.19**
[^{3}H]Taxol	2.95 ± 0.19	4.5 ± 0.09*	5.54 ± 0.05	7.13 ± 0.36*	ND	ND	ND	ND

Data are presented as percentage of total activity added to basal or apical side (mean ± SEM of three determinations each). ND, not determined. *, $P < 0.05$; **, $P < 0.001$.

sides resulted in significantly enhanced apical-to-basal permeation and diminished basal-to-apical permeation, consistent with a Pgp-mediated barrier located on the apical surface. GF120918 also enhanced by 2-fold the final cell-associated content of [^{3}H]Taxol (Table 1). Taken together, these vectorial differences in translocation of ^{99m}Tc-sestamibi and [^{3}H]Taxol indicate that Pgp functionally confers an apical drug-permeation barrier, whereas MRP functionally confers an opposing basolateral drug-permeation barrier to CP epithelial cells.

DISCUSSION

Our results identify *MDR1* Pgp and MRP in the epithelia of CP and directly show that these transporters participate in a bipolar permeation barrier for selected drugs crossing the B-CSF barrier. These data complement reports of preferential trafficking of substrates toward the apical surface in epithelial cells transfected with *MDR1* Pgp (41) or the basolateral surface in epithelia transfected with MRP (42) and have further implications for transporter-mediated intracellular trafficking of substrates in CP epithelial cells.

From the perspective of the CNS as a drug sanctuary, Pgp is known to contribute to the drug-permeation barrier in cerebral capillary endothelial cells (7); however, our findings indicate that MRP, not Pgp, contributes to the basolateral broad-specificity drug-permeation barrier in CP. In contrast to sites such as liver and kidney, wherein Pgp is reported to have an excretory function in protecting the organism against xenobiotics, in CP epithelia, apical localization of Pgp paradoxically seems to prevent trafficking of certain substrates out of the CSF. Here, Pgp at the B-CSF barrier opposes the action of Pgp at the BBB in elimination of organic cations and xenobiotics from the CNS. Also, whether natural substrates putatively transported by Pgp, such as phospholipids or other ions, actually are secreted into CSF or, conversely, other functions attributed to Pgp, such as enhancement of cholesterol uptake and esterification (43), occur within CP epithelia and contribute to CNS sterol homeostasis remains to be determined. In either case, it is likely that these ATP-binding cassette transporters function in association with other broad-specificity transporters, such as the organic anion-transport protein family in CP (11) and other tissues (44).

The coordinated expression of Pgp, MRP, and organic anion-transport proteins in CP underscores the complexity of CNS substrate homeostasis and may provide insight into the differential translocation of organic cations, drugs, sterols, lipids, and conjugated anions, such as leukotriene C_4, into and out of the brain. In addition, CNS pharmacokinetics of drugs comprising the multidrug resistance phenotype, including chemotherapeutic agents, selected antibiotics, antidepressants, antipsychotics (45), and HIV protease inhibitors (46), are likely to be impacted by the relative activity of these transporters expressed at each barrier. Our results suggest that maximizing the CNS penetration of these therapeutic agents may require at the least concurrent blockade of both Pgp and MRP.

This paper is in memory of Alfred P. Wolf. We thank Gary and Kathryn Luker for insightful discussions, Carolyn Crankshaw for technical assistance, Henry Royal and Delynn Silvestros for support with SPECT imaging, Marilyn Levy for electron microscopy, and Gary Kruh for providing NIH 3T3 MRP cells. This work was supported by U.S. Department of Energy Grant DE-FG02-94ER61885 and National Institutes of Health Grant RO1 CA65735.

1. Gottesman, M. M. & Pastan, I. (1993) *Annu. Rev. Biochem.* **62,** 385–427.
2. Cordon-Cardo, C., O'Brien, J. P., Casals, D., Rittman, G. L., Biedler, J. L., Melamed, M. R. & Bertino, J. R. (1989) *Proc. Natl. Acad. Sci. USA* **86,** 695–698.
3. Cole, S. P. C., Bhardwaj, G., Gerlach, J. H., Mackie, J. E., Grant, C. E., Almquist, K. C., Stewart, A. J., Kurz, E. U., Duncan, A. M. V. & Deeley, R. G. (1992) *Science* **258,** 1650–1654.
4. Flens, M. J., Zaman, G. J. R., van der Valk, P., Izquierdo, M. A., Schroeijers, A. B., Scheffer, G. L., van der Groep, P., de Haas, M., Meijer, C. J. L. M. & Scheper, R. J. (1996) *Am. J. Pathol.* **148,** 1237–1247.
5. Zaman, G. J. R., Versantvoort, C. H. M., Smit, J. J. M., Eijdems, W. H. M., de Haas, M., Smith, A. J., Broxterman, H. J., Mulder, N. H., de Vries, E. G. E., Baas, F., *et al.* (1993) *Cancer Res.* **53,** 1747–1750.
6. Schinkel, A., Smit, J., van Tellingen, O., Beijnen, J., Wagenaar, E., van Deemter, L., Mol, C., van der Valk, M., Robanus-Maandag, E., te Riele, H., *et al.* (1994) *Cell* **77,** 491–502.
7. Schinkel, A., Mayer, U., Wagenaar, E., Mol, C., van Deemer, L., Smit, J., van der Valk, M., Voordouw, A., Spits, H., van Tellingen, O., *et al.* (1997) *Proc. Natl. Acad. Sci. USA* **94,** 4028–4033.
8. Keep, R. F. & Jones, H. C. (1990) *Dev. Brain Res.* **56,** 47–53.
9. Spector, R. & Johanson, C. (1989) *Sci. Am.* **261** (5)**,** 68–74.
10. Spector, R. (1990) *Pharmacology* **40,** 1–7.
11. Angeletti, R., Novikoff, P., Juvvadi, S., Fritschy, J., Meier, P. & Wolkoff, A. (1997) *Proc. Natl. Acad. Sci. USA* **94,** 283–286.
12. Lautier, D., Canitrot, Y., Deeley, R. & Cole, S. (1996) *Biochem. Pharmacol.* **52,** 967–977.
13. Luker, G., Rao, V., Crankshaw, C., Dahlheimer, J. & Piwnica-Worms, D. (1997) *Biochemistry* **36,** 14218–14227.
14. Breuninger, L. M., Paul, S., Gaughan, K., Miki, T., Chan, A., Aaronson, S. A. & Kruh, G. D. (1995) *Cancer Res.* **55,** 5342–5347.
15. Lorico, A., Rappa, G., Finch, R., Yang, D., Flavell, R. & Sartorelli, A. (1997) *Cancer Res.* **57,** 5238–5242.
16. Georges, E., Bradley, G., Gariepy, J. & Ling, V. (1990) *Proc. Natl. Acad. Sci. USA* **87,** 152–156.
17. Esterle, T. M. & Sanders-Bush, E. (1992) *J. Neurosci.* **12,** 4775–4782.
18. Southwell, B. R., Duan, W., Alcorn, D., Brack, C., Richardson, S. J., Kohrle, J. & Schreiber, G. (1993) *Endocrinology* **133,** 2116–2126.
19. Crook, R. B., Kasagami, H. & Prusiner, S. B. (1981) *J. Neurochem.* **37,** 845–854.
20. Shyng, S.-L., Heuser, J. & Harris, D. (1994) *J. Cell Biol.* **125,** 1239–1250.
21. Piwnica-Worms, D., Rao, V., Kronauge, J. & Croop, J. (1995) *Biochemistry* **34,** 12210–12220.
22. Pirro, J., DiRocco, R., Narra, R. & Nunn, A. (1994) *J. Nucl. Med.* **35,** 1514–1519.
23. Paxinos, G. & Watson, C. (1986) *The Rat Brain in Stereotaxic Coordinates* (Academic, Sydney).
24. Benveniste, H. & Hansen, A. (1991) in *Microdialysis in the Neurosciences*, eds. Robinson, T. E. & Justice, J. B. (Elsevier, Amsterdam), pp. 81–102.
25. Robinson, T. E. & Wishaw, I. Q. (1988) *Brain Res.* **450,** 209–224.
26. Andersson, J., Sundin, A. & Valind, S. (1995) *J. Nucl. Med.* **36,** 1307–1315.
27. Crankshaw, C. & Piwnica-Worms, D. (1996) *J. Nucl. Med.* **37,** 247P.
28. Hendrikse, N., Franssen, E., van der Graaf, W., Meijer, C., Piers, D., Vaalburg, W. & de Vries, E. (1998) *Br. J. Cancer* **77,** 353–358.
29. O'Tuama, L. A., Treves, S. T., Larar, J. N., Packard, A. B., Kwan, A. J., Barnes, P. D., Scott, R. M., Black, P. M., Madsen, J. R., Goumnerova, L. C., *et al.* (1993) *J. Nucl. Med.* **34,** 1045–1051.
30. Hyafil, F., Vergely, C., Du Vignaud, P. & Grand-Perret, T. (1993) *Cancer Res.* **53,** 4595–4602.
31. Germann, U., Ford, P., Schlakhter, D., Mason, V. & Harding, M. (1997) *Anticancer Drugs* **8,** 141–155.
32. Mickisch, G. H., Pai, L. H., Pastan, I. & Gottesman, M. M. (1992) *Cancer Res.* **52,** 4427–4432.
33. Flens, M. J., Izquierdo, M. A., Scheffer, G. L., Fritz, J. M., Meijer, C. J. L. M., Scheper, R. J. & Zaman, G. J. R. (1994) *Cancer Res.* **54,** 4557–4563.
34. Hipfner, D. R., Almquist, K. C., Stride, B. D., Deeley, R. G. & Cole, S. P. C. (1996) *Cancer Res.* **56,** 3307–3314.
35. Villalobos, A., Parmelee, J. & Pritchard, J. (1997) *J. Pharmacol. Exp. Ther.* **282,** 1109–1116.
36. Abbaszadegan, M., Cress, A., Futscher, B., Bellamy, W. & Dalton, W. (1996) *Cancer Res.* **56,** 5435–5442.
37. Jones, T., Zamboni, R., Belley, M., Champion, E., Charette, L., Ford-Hutchinson, A., Frenette, R., Gauthier, J.-Y., Leger, S., Masson, P., *et al.* (1989) *Can. J. Physiol. Pharmacol.* **67,** 17–28.
38. Akiyama, S. I., Fojo, A., Hanover, J. A., Pastan, I. & Gottesman, M. M. (1985) *Somatic Cell Mol. Genet.* **11,** 117–126.
39. Podda, S., Ward, M., Himelstein, A., Richardson, C., de la Flor-Weiss, E., Smith, L., Gottesman, M., Pastan, I. & Bank, A. (1992) *Proc. Natl. Acad. Sci. USA* **89,** 9676–9680.
40. Zaman, G. J. R., Flens, M. J., Van Leusden, M. R., De Haas, M., Mulder, H. S., Lankelma, J., Pinedo, H. M., Scheper, R. J., Baas, F., Broxterman, H. J., *et al.* (1994) *Proc. Natl. Acad. Sci. USA* **91,** 8822–8826.
41. van Helvoort, A., Smith, A. J., Sprong, H., Fritzsche, I., Schinkel, A. H., Borst, P. & van Meer, G. (1996) *Cell* **87,** 507–517.
42. Evers, R., Zaman, G. J., van Deemter, L., Jansen, H., Calafat, J., Oomen, L. C. J. M., Oude Elferink, R. P. J., Borst, P. & Schinkel, A. H. (1996) *J. Clin. Invest.* **97,** 1211–1218.
43. Luker, G., Nilsson, K., Covey, D. & Piwnica-Worms, D. (1999) *J. Biol. Chem.* **274,** 6979–6991.
44. Bergwerk, A., Shi, X., Ford, A., Kanai, N., Jacquemin, E., Burk, R., Bai, S., Novikoff, P., Stieger, B., Meier, P., *et al.* (1996) *Am. J. Physiol.* **271,** G231–G238.
45. Ford, J. M. & Hait, W. N. (1990) *Pharmacol. Rev.* **42,** 155–199.
46. Kim, R. B., Fromm, M. F., Wandel, C., Leake, B., Wood, A. J. J., Roden, D. M. & Wilkinson, G. R. (1998) *J. Clin. Invest.* **101,** 289–294.